

PALMPRINT VERIFICATION USING CONSISTENT ORIENTATION CODING

Zhenhua Guo¹, Wangmeng Zuo², Lei Zhang¹, David Zhang¹

¹Biometrics Research Centre, Department of Computing, the Hong Kong Polytechnic University

²School of Computer Science and Technology, Harbin Institute of Technology

ABSTRACT

Developing accurate and robust palmprint verification algorithms is one of the key issues in automatic palmprint recognition systems. Recently, orientation based coding algorithms, such as Competitive Code (CompCode) and Orthogonal Line Ordinal Features (OLOF), have been proposed and have been attracting much research attention. Such algorithms could achieve high accuracy with high feature matching speed for real time implementation. By investigating the relationship between these two different coding schemes, we propose in this paper a feature-level fusion scheme for palmprint verification. Only the stable features which are consistent between the two codes are extracted for matching. The experimental results on the public palmprint database show that the proposed fusion code could achieve at least 14% EER (Equal Error Rate) reduction compared with either of the original codes.

Index Terms—palmprint verification, feature-level fusion, orientation coding

1. INTRODUCTION

As a substitution or complementary technology for traditional personal authentication methods, biometric techniques are becoming more and more popular in public security applications. Biometrics is the study of methods for uniquely recognizing humans based upon one or more intrinsic physical or behavioral traits, including the extensively studied fingerprint, face, iris, speech, hand geometry, etc [1]. Palmprint authentication as an emerging biometrics technology has been drawing much attention in both academic and industry societies [2-10] because it owns many merits, such as robustness, user-friendliness and cost-effectiveness.

Palmprint is composed of three main kinds of features: principal lines (usually three dominant lines on the palm), wrinkles (weaker and more irregular lines) and minutia (ridge and valley features which are similar to those in fingerprint images) [2]. Unlike fingerprint which requires a high resolution (about 500dpi) to capture clear minutia features, the principal lines and wrinkles in a palmprint could be captured under a low resolution (<100dpi) and they could provide enough discriminatory information for

personal identification. Fig. 1-a shows the Region of Interest (ROI) of a palmprint sample image [2].

Competitive Code (CompCode) [8] and Orthogonal Line Ordinal Features (OLOF) [9] are state-of-the-art algorithms for palmprint verification because they could achieve very high accuracy with a high matching speed. Taking palm lines as negative lines, Kong and Zhang [8] proposed to extract and code the orientation of palm lines for palmprint verification. They applied six Gabor filters to the image and selected one main orientation for each local region. Sun et al. [9] proposed a new palmprint representation. They compared two elongated line-like image regions, which are orthogonal in orientation, and then assigned one bit feature code. Three bits are then obtained by using three different orientated ordinal filters. Two example maps of CompCode and OLOF extracted from Fig. 1-a are shown in Fig. 1-b and Fig. 1-c.

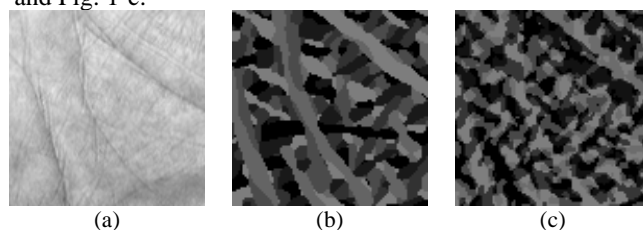


Fig.1 (a) The ROI of a sample palmprint image and the extracted (b) CompCode map and (c) OLOF map. Different features are represented by using different gray values.

From Fig. 1, we can see that the OLOF and CompCode maps of the same palmprint are different but both of them have clear representation of principal lines and wrinkles. Since principal lines and wrinkles are the most stable and robust features in low resolution palmprint images, it inspires us to develop a feature level fusion scheme to further enhance those stable features for a more robust feature extraction. After investigating the correlation between OLOF and CompCode, in this paper, we propose such a feature level fusion scheme according to the consistency between the two different codes.

The rest of the paper is organized as follows. Section 2 briefly reviews CompCode and OLOF. Section 3 analyzes the correlation between them and then fuses them. Section 4 verifies the proposed scheme on a large public palmprint database. Finally, Section 5 concludes the paper.

2. BRIEF REVIEW OF COMPCODE AND OLOF

2.1. CompCode [8]

To extract the orientation information from palm lines, CompCode uses six real parts of the neurophysiology-based Gabor filters ψ_θ , which is defined as:

$$\psi(x, y, \omega, \theta) = \frac{\omega}{\sqrt{2\pi\kappa}} e^{-\frac{\omega^2}{8\kappa^2}(4x'^2+y'^2)} \left(e^{i\omega x'} - e^{-\frac{\kappa^2}{2}} \right) \quad (1)$$

where $x' = (x - x_0) \cos \theta + (y - y_0) \sin \theta$, $y' = -(x - x_0) \sin \theta + (y - y_0) \cos \theta$. (x_0, y_0) is the center of the function; ω is the radial frequency in radians per unit length and θ is the orientation of the Gabor function in radians. κ is defined by $\kappa = \sqrt{2 \ln 2} \left(\frac{2^\delta + 1}{2^\delta - 1} \right)$, where δ is the half-amplitude bandwidth of the frequency response.

For each pixel, six filters with $\theta_j = j\pi/6$, $j=\{0,1,2,3,4,5\}$, are applied. According to palm lines' property, CompCode selects:

$$I_{CompCode} = \arg \min_j (I(x, y) * \psi_R(x, y, \omega, \theta_j)) \quad (2)$$

as the orientation at position (x, y) of image I . To implement real-time palmprint recognition, CompCode uses three bits to represent each orientation [8]. An angular distance based on Hamming distance is used for distance comparison:

$$D(P, Q) = \frac{\sum_{y=1}^M \sum_{x=1}^N \sum_{i=1}^3 (P_i^b(x, y) \otimes Q_i^b(x, y))}{3 * M * N} \quad (3)$$

where P and Q are two CompCodes. $P_i^b(Q_i^b)$ is the i^{th} bit plane of $P(Q)$ and \otimes is bitwise exclusive OR.

2.2. OLOF [9]

OLOF uses an orthogonal line ordinal filter to compare two orthogonal line-like palmprint image regions. The filter is as follows:

$$OF(\theta) = f(x, y, \theta) - f(x, y, \theta + \frac{\pi}{2}) \quad (4)$$

$$f(x, y, \theta) = e^{-\left(\frac{x \cos \theta + y \sin \theta}{\sigma_x}\right)^2 - \left(\frac{x \cos \theta - y \sin \theta}{\sigma_y}\right)^2}$$

where θ denotes the orientation of the 2D Gaussian filter, σ_x and σ_y are the horizontal and vertical scales of the filter.

Similar to CompCode, three ordinal filters $OF(0)$, $OF(\pi/6)$ and $OF(\pi/3)$ (refer to Fig. 2) are applied to

each pixel and a three-bit ordinal code is obtained according to the sign of the filtering results. The matching metric on Hamming distance is defined the same as Eq. 3.



Fig.2 Ordinal filters.

An integer value could be computed with the three-bit code using the following formula:

$$I_{OLOF} = s(W(0)) * 1 + s(W(\pi/6)) * 2 + s(W(\pi/3)) * 4 \quad (5)$$

$$s(x) = \begin{cases} 1, & x \geq 0 \\ 0, & x < 0 \end{cases}$$

where $W(\theta)$, $(\theta = 0, \pi/6, \pi/3)$ is the filter response after convolving $OF(\theta)$ with the input image.

3. CONSISTENT ORIENTATION CODE

CompCode and OLOF could achieve high accuracy. Although they use different coding strategies, they have some consistency in representing palm stable features, as can be seen in Fig. 1. After investigating the correlation between these two codes, we propose a feature-level fusion scheme, namely consistent orientation code, in this section.

3.1. Correlation between CompCode and OLOF

Although OLOF is not designed as an orientation estimator, it can be used to represent a line's orientation like the CompCode does. Suppose there is a straight dark line in a white background as shown in Fig. 3-a. We rotate Fig. 3-a counterclockwise by different angles, e.g. from 1 to 180 degree with 1 degree interval (referring to Fig. 3-b ~ Fig. 3-f for examples). The associated $I_{CompCode}$ and I_{OLOF} code maps are plotted in Fig. 4. It can be seen that there is clear correlation between CompCode and OLOF for this simple line image. Taking Fig. 3-a for example, since the dark line is closer to the "+" part than the "-" part of $OF(0)$ and $OF(\pi/6)$ (referring to Fig. 2), the filtering outputs of $OF(0)$ and $OF(\pi/6)$ will be smaller than 0, while the filtering output by $OF(\pi/3)$ will be bigger than 0. So according to Eq. 5, I_{OLOF} is equal to 4. Meanwhile, the competitive code, $I_{CompCode}$, of this line will be 3 because $\psi_R(x, y, \omega, \theta_{\pi/2})$ has the minimal value.

For real palmprint image, however, the structure is much more complex. For example, in a local region, there may have non-straight lines, weak lines and even multiple lines. Table 1 shows the co-occurrence percentage between

CompCode and OLOF on a portion of the PolyU database [11] (first six images of each palm, totally $386 \times 6 = 2316$ images). As we can see from Table 1, there is a strong correlation between CompCode and OLOF but it is hard to find a direct mapping function between them. Intuitively, the consistent parts between the two codes will reflect the most stable and important features in the palmprint, while the inconsistent parts may come from noise and the unstable features in the palmprint. Therefore, it inspires us to consider a feature-level fusion scheme to extract the consistent features in the two codes and remove the non-consistent part so that the recognition accuracy could be further improved.

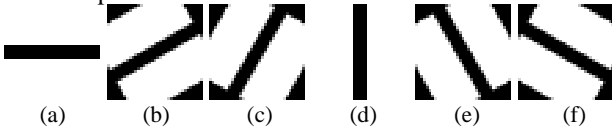


Fig. 3 An image with a straight line and its rotated image. (a) is the original image and (b)-(f) are the 30, 60, 90, 120 and 150 degree counterclockwise rotated versions of (a).

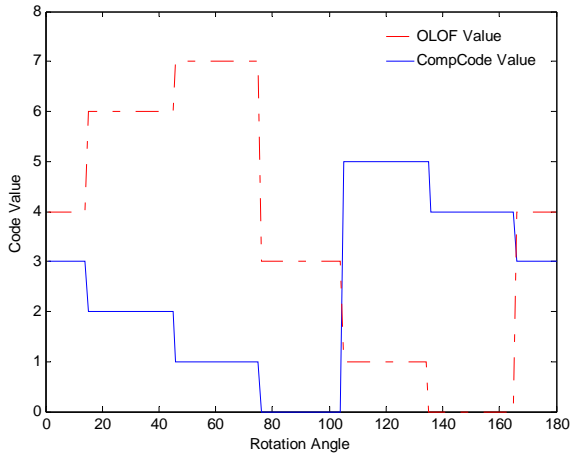


Fig. 4 Rotation angle vs. Coding value of OLOF and CompCode.

Table 1. Co-occurrence percentage of CompCode and OLOF on partial PolyU palmprint database.

CompCode \ OLOF	0	1	2	3	4	5
0	0.4220	0.1733	0.4559	3.7009	8.0190	3.7362
1	3.7728	0.4797	0.1955	0.4171	3.9493	8.4655
2	0.0055	0.0376	0.0056	0.0391	0.0063	0.0377
3	7.2229	4.2097	0.4286	0.1922	0.4390	4.0738
4	0.1733	0.3500	3.6424	7.4978	3.5182	0.3580
5	0.0388	0.0063	0.0401	0.0062	0.0393	0.0070
6	0.4398	3.8072	8.2218	3.6534	0.4342	0.1822
7	3.7095	8.4643	3.8915	0.4063	0.1823	0.4450

3.2. Proposed Fusion Scheme

Table 1 shows that around half (47.8912%, the sum of underscored number) of the CompCode and OLOF codes has a strong consistency. Fig. 5-a) shows the strong

consistent part between CompCode and OLOF extracted from Fig. 1. As we can see, the strong consistent part is mainly from principal lines and strong wrinkles.

However, the strong consistency is less than 50 percent. If we keep this part only, we may not have enough discriminate information for verification. On the other hand, if we regard that the part highlighted with bold number in Table 1 has a relatively weak consistency, the valid portion is more than 90 percents (93.5562%, the sum of bold number). The weak consistency can contribute additional information while some unstable parts are removed. Fig. 5-b) shows the weak consistent part. We can see that weak consistency contains almost all of principal lines and wrinkles.

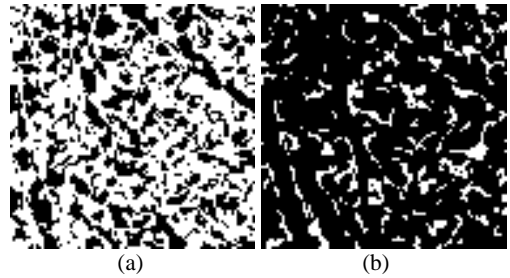


Fig. 5 (a) Strong consistent part (in black color) between Fig. 1-b and Fig. 1-c; and (b) weak consistent part (including strong consistent part) between Fig. 1-b and Fig. 1-c.

Here, we propose two different fusion schemes: Strong Consistent Fusion (keep strong consistent part only) and Weak Consistent Fusion (keep weak consistent part only). The distance for the proposed fusion scheme is defined as:

$$D(P, Q) = \frac{\sum_{y=0}^M \sum_{x=0}^N \sum_{i=1}^3 (P_M(x, y) \cap Q_M(x, y)) \cap (P_i^b(x, y) \otimes Q_i^b(x, y))}{3 \sum_{y=0}^M \sum_{x=0}^N P_M(x, y) \cap Q_M(x, y)} \quad (6)$$

where \cap is bitwise AND operation, P_M and Q_M are the corresponding masks to indicate whether this pixel is kept according to the consistency criteria.

4. EXPERIMENT RESULTS

To validate our proposed consistent orientation coding scheme, we tested it on a large public palmprint database [11]. The database contains 7752 grayscale images collected from 386 palms. Those palmprint images were collected in two sessions with an average time interval of 69 days. Around 10 images per palm were captured per session.

The central part (128*128) of the palm image is cropped by using an ROI extraction algorithm similar to [2]. To further reduce the influence of imperfect ROI extraction, we translate the feature map vertically and horizontally from -4 to 4 when matching it with the feature maps in the database. The minimal distance obtained by translated matching is regarded as the final distance. Compared with

originally used searching range, -2 to 2 [8-9], here the searching range is increased for better accuracy.

In palmprint verification test, each palmprint image is matched with all the other palmprint images in the database. A match is counted as correct if the two palmprint images are from the same palm; otherwise, the match is counted as incorrect. The total number of matches is $7752 \times 7751 / 2 = 30,042,876$, and among them there are 74,068 correct matchings. The index of equal error rate (EER), a point when false accept rate (FAR) is equal to false reject rate (FRR), is used to evaluate the performance. In addition, the discriminating index d' (d-prime) [12] is computed for reference.

The curves of receiver operating characteristic (ROC) for the original CompCode, OLOF and the proposed two fusion codes are plotted in Fig. 6. The indices of EER and d' are listed in Table 2. Since we increased the matching range and made some optimization on ROI extraction, such as some morphological operations after binarization to overcome the broken finger problem caused by shading, the result of CompCode is better than what was reported in the original publication [8].

Table 2 Accuracy comparison.

Algorithm	EER	d'	FRR (when FAR= $3.3 \times 10^{-6}\%$)
CompCode	0.0379	5.4122	1.2273
OLOF	0.0553	6.0301	1.5621
Strong Consistent	0.0987	7.0468	4.4108
Weak Consistent	0.0324	5.6925	0.7858

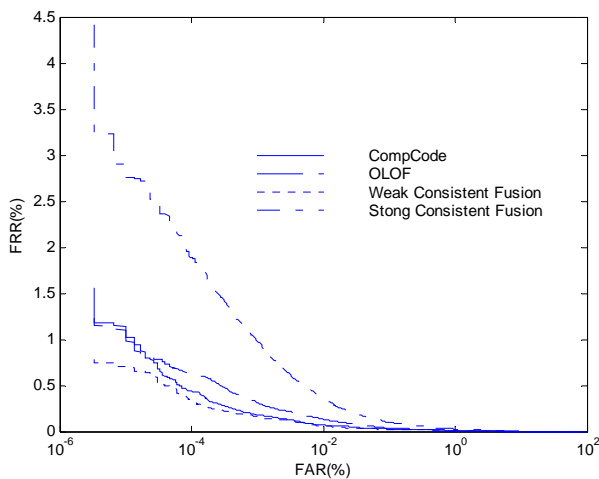


Fig. 6 Verification performance comparison.

From the experimental results, we can see that the weak consistent fusion scheme could achieve much better performance than the original CompCode and OLOF codes, which is largely attributed to the removal of unstable or non-robust information. Although strong consistent fusion could get the highest d' , it also has the highest EER value. It validates that d' is not highly correlated with ROC curve. The proposed method achieves at least 14% (0.0379%-

>0.0324%) EER reduction and correctly reject more than 1,600 (0.0055%*29,968,808) impostor attempts compared with either of the original codes.

5. CONCLUSION

In this paper, we analyzed the correlation between two state-of-the-art palmprint verification algorithms: CompCode and OLOF. Based on the observations, a feature level fusion scheme by exploiting the consistency between the two codes was proposed. The experimental results on the public database showed that by keeping the consistent orientation features, the palmprint verification accuracy could be improved significantly compared with either the original CompCode or OLOF algorithm.

6. ACKNOWLEDGEMENT

This work is partially supported by the Hong Kong RGC General Research Fund (PolyU 5351/08E).

7. REFERENCES

- [1] Jain, A., Bolle, R., and Pankanti, S. (eds.), *Biometrics: Personal Identification in Networked Society*, Kluwer Academic Publishers, Boston, 1999.
- [2] Zhang, D., Kong, W. K., You, J., and Wong, M., "Online palmprint identification," *IEEE Trans. Pattern Analysis and Machine Intelligence*, vol. 25, pp. 1041-1050, 2003.
- [3] Ribaric, S., and Fratric, I., "A biometric identification system based on eigenpalm and eigenfinger features," *IEEE Trans. on Pattern Analysis and Machine Intelligence*, vol. 27, pp. 1698-1709, 2005.
- [4] Han, C.-C., Cheng, H.-L., Lin, C.-L., and Fan, K.-C., "Personal authentication using palm-print features," *Pattern Recognition*, vol. 36, pp. 371-381, 2003.
- [5] Connie, T., Andrew, T., and Goh, K., "An automated palmprint recognition system," *Image and Vision Computing*, vol. 23, pp. 501-505, 2005.
- [6] Hu, D., Feng, G., and Zhou, Z., "Two-dimensional locality preserving projections (2DLPP) with its application to palmprint recognition," *Pattern Recognition*, vol. 40, pp. 339-342, 2007.
- [7] Wang, J., Yau, W., Suwandy, A., and Sung, E., "Person recognition by fusing palmprint and palm vein images based on "Laplacianpalm" representation," *Pattern Recognition*, vol. 41, pp. 1531-1544, 2008.
- [8] Kong, A., and Zhang, D., "Competitive coding scheme for palmprint verification," *International Conference on Pattern Recognition*, pp. 520-523, 2004.
- [9] Sun Z., Tan T., Wang Y., and Li S. Z., "Ordinal palmprint representation for personal identification," *IEEE Computer Society Conference on Computer Vision and Pattern Recognition*, pp. 279-284, 2005.
- [10] Jia, W., Huang, D.-S., and Zhang, D., "Palmprint verification based on robust line orientation code," *Pattern Recognition*, vol. 41, pp. 1521-1530, 2008.
- [11] PolyU Palmprint Database, <http://www.comp.polyu.edu.hk/~biometrics>.
- [12] Daugman J., and Williams G., "A proposed Standard for biometric decidability," *Proc. CardTech/SecureTech Conference*, pp. 223-234, 1996.